



## Combined DEM and SPH simulation of ball milling

M. Jahani Chegeni

Faculty of Mining, Petroleum & Geophysics Engineering, Shahrood University of Technology, Shahrood, Iran

Received 13 August 2018; received in revised form 5 October 2018; accepted 13 November 2018

### Keywords

*Simulation*

*Ball Mill*

*DEM*

*SPH*

*DEM-SPH Coupling*

### Abstract

A deeper understanding of the milling operation of ball mills helps mineral processing engineers to control and optimize them, and therefore, reduce their consuming power. In this work, the milling operation of ball mills is investigated using two methods, i.e. DEM and combined DEM-SPH. First, a pilot scale ball mill with no lifter is simulated by both methods. Then another pilot scale ball mill with eight rectangle lifters is simulated again by both methods. The effects of lifters on ball shoulder and toe points as well as on creation of cascading and cataracting movements for balls are studied by both methods. At the present time, there is not enough measured data available for dense slurries interacting with the coarse particulates available in the public domain that can be used adequately to validate these types of predictions. The results obtained indicated that fluid slurry in the mill lowered the charge shoulder by about 28 cm and 25 cm in the no-lifter and eight-lifter cases, respectively. However, it raised the charge toe by about 36 cm and 6 cm in the no-lifter and eight-lifter cases, respectively.

### 1. Introduction

The mineral processing industry could save about 70% of the power involved in grinding processes if this power was reduced to its practical minimum power consumption [1]. In this context, achieving a more efficient grinding in ball mills is an important issue since they have a low efficiency rate, partially due to the lack of creation of cascading and cataracting movements for balls and inappropriate shoulder and toe points [2].

For a given amount of balls, if the mill rotation speed is higher than its critical speed, the balls stick to the mill wall, and the grinding operation does not happen. On the other hand, if the mill speed is between 80% and 100% of its critical speed, the suitable toe points are not created, and the grinding energy is used to hit the balls with the mill wall. However, if the mill speed is about 80% of its critical speed, the appropriate shoulder and toe points as well as the cascading and cataracting movements are created, which result in a better grinding. In this case, the dominant mechanism is impact, and the abrasion mechanism is not very effective. At speeds much slower than the critical

speed, the cascading and cataracting movements gradually disappear and the balls roll over each other. In this case, grinding is not optimal and the abrasion mechanism plays a more effective role [2]. Among the other effective factors on creating cascading and cataracting movements in mills, lifters can be mentioned. Lifters cause the balls to climb to a higher elevation and prevent their slipping [2].

Simulation has become a common tool in the design and optimization of industrial processes [3-5]. The continuous increase in the computing power is now enabling researchers to implement the numerical methods that do not focus on the granular assembly as an entity but rather deduce its global characteristics from observing the individual behavior of each grain [6]. Due to their highly discontinuous nature, one should expect that granular media require a discontinuous simulation method. Indeed, to date, the Discrete Element Method (DEM) is the leading approach to those problems [6]. Due to its inherent advantages in analyzing granular materials, DEM

has been developed rapidly in the recent decades, and is used widely in mineral processing engineering [7-9]. Since in the mineral processing industry we deal with the pulp, i.e. a combination of solid and fluid phases, and DEM only has the ability to simulate solid particles, for making realistic simulations, its combination with other methods such as Computational Fluid Dynamics (CFD) and Smoothed Particle Hydrodynamics (SPH) which can simulate the fluid phase is essential. In the next paragraph, the SPH method and its combination with the DEM method, i.e. the DEM-SPH coupling method, will be introduced.

Prediction of slurry flow in a ball mill is a particularly difficult computational challenge. The rotating mill geometry and the requirement to resolve the free surfaces of the fluid make solution using grid-based Eulerian flow solvers problematic. In particular, the fragmenting flow of the many thin streams of fluid passing through the potentially hundreds of grate holes is prohibitive. The fluid method most suited to this application is Smoothed Particle Hydrodynamics (SPH) since it naturally allows the prediction of complex splashing and fragmenting free surface flow for the fluid in complex rotating mill geometries [10]. The problem of slurry transport in ball mills requires both the ability to model the particulate solids and the slurry. The methodology utilized here to explore the flow of slurry in mills uses a sequential DEM-SPH model. The process has three key steps:

- Perform a DEM simulation to predict the particle flow and average the particle data onto a cylindrical grid to obtain a steady state volume fraction and velocity distributions that then well characterize the charge.

- Supply the continuum porosity and velocity information from the DEM simulation to the SPH code. The mill geometry used by the two codes is the same but the charge representation changes from discrete to continuous.

- Perform an SPH simulation of the distribution of slurry in this charge using a supplied slurry viscosity and a Darcy law porous media drag based upon the porosity and velocity distributions within the charge [11].

For processes in which slurry flow does not dominate the coarse particle behavior, a one-way coupled model can be used. With this approach, a dynamic “porous media” can be characterized from the DEM analysis by averaging the particles onto a fixed data collection grid. This dynamic porous medium is included in the fluid model to

represent the average effect of the solid component of the charge. The fluid method most suited to this application is again the SPH method since:

- It naturally allows prediction of complex splashing and fragmenting free surface flow for the fluid in complex rotating mill geometries.

- It supports coupling of the porous media model to the fluid in order to predict fluid flow within the dynamically moving particulate matrix [10].

This sequential model is possible for ball mill because the particulate flow is in the steady state and the balls represented in DEM are only weakly affected by the slurry motion. The slurry motion through the charge is dominated by the flow of the balls in the charge. Therefore, this one-way coupling is capable of capturing the majority of key physics required to predict the slurry behavior. It allows prediction of slurry distribution within the mill (both in the radial and axial directions) as well as axial transport including discharge through the grates and flow in the pulp lifters and on the discharge end. The one-way coupling means fluid affects particle motion but particle motion does not affect fluid motion. That is why it is called one-way. Inclusion of the effect of particle motion on fluid motion (two-way coupling), effect of particle disturbance of the fluid that locally affects another particle motion (three-way coupling), and effect of particle collision on motion of both particles (four-way coupling or a fully coupled SPH-DEM model) is not currently possible with the existing hardware in Iran.

So far, little works have been done in the field of simulation of ball mills using the DEM and SPH coupling. One of the newest works is related to Sinnott et al. [12], in which an overflow ball mill discharge and trommel flow has been simulated using the combined DEM and SPH method. The present work has some similarities and differences with that one as follow: in our simulation, we used the one-way coupling method in which continuous fluid affects particle motion. However, in the one-way coupling, particle motion does not affect fluid motion. Also we concluded that in both the no-lifter and 8-lifter ball mills, the addition of slurry caused to lower the charge shoulder positions but it raised the charge toe positions. In the work carried out by Sinnott et al. [12], in the mill grinding chamber, the addition of slurry was found to lower the charge shoulder and toe positions due to drag forces on the media as well as produce a large slurry pool above the toe. Also

they used a two-way coupling method in which particle motion also affected fluid motion. In a near future, we are going to perform two-way coupling simulations or even for more reliable simulations four-way coupling.

To control, optimize, and reduce the ball mill power consumption, mineral processing engineers must obtain enough information about their operation conditions. One of the most effective techniques is the use of computer simulations. Computer simulations using methods such as DEM or its coupling with other methods such as SPH (DEM-SPH) can be effective to find the optimal speed of ball mills, and as a result, creating appropriate shoulder and toe points in them as well as creating cascading and cataracting movements. In this paper, the DEM and combined DEM-SPH techniques are introduced and used to simulate the milling operation of ball mills. Two pilot scale ball mills with no lifter and with 8-lifter were simulated by both methods. The effects of lifters on ball shoulder and toe points, on creation of cascading and cataracting movements for balls, and milling operation are studied by both methods. In the DEM method, only the solid phase (balls) is simulated but in the DEM-SPH method, both the solid phase and the fluid phase (balls/slurry) are simulated, that is, the effect of the fluid phase on the movement of the balls is also simulated.

In this research work, for the first time in Iran, mineral processing equipment (ball mill) was simulated by the DEM and SPH coupling methods. In the previous research works, the DEM and CFD coupling methods were commonly used but in this work, the SPH method, which is a mesh-free method, replaces the CFD method, which is much more effective than CFD for simulating the turbulent flows (like what is seen in the ball mills). The coupling of these two methods adds the ability to simulate the fluid phase to the solid phase, which can be done by the DEM method. For the first time, the effect of the fluid phase on the shoulder and toe points was simulated for pilot scale ball mills without lifter and with eight lifters.

## 2. Simulation methods

### 2.1. Using DEM to predict particle flow

The Discrete Element Method (DEM) is a numerical technique used to predict the behavior of collision-dominated particle flows. Each particle in the flow is tracked, and all collisions between particles and between particles and boundaries are modeled. DEM is a powerful

numerical tool for simulating the mechanical behavior of systems with a large number of particles based on the motion and interaction of particles and their representation as rigid geometric bodies, commonly having a spherical shape [13, 14]. Simulations with spherical particles can include millions of particles, and using non-spherical particles is still not an easy task. For spherical particles, the geometry is described by the radius, and the interaction forces can easily be calculated by contact laws like the Hertzian contact law. For non-spherical particles, the geometry representation and calculation of contact forces are much more complex [13, 15]. DEM is based upon the Lagrangian approach, and treats granular materials as an assemblage of distinct particles, each governed by physical laws [16, 17]. Each particle interacts with its neighbors through particle-to-particle contacts, which can be formed or broken at each time step [14, 16, 18-20]. In the recent years, the drastic increase in affordable computational power has allowed DEM simulations to become a versatile tool for industrial applications [21]. The recent advances in discrete element modeling have resulted in this method becoming a useful simulation tool that can provide detailed information not easily measured during experiments [22]. With the maturing of DEM simulation, it has now become possible to run simulations of millions of particles with complex shapes and inter-particle cohesive forces in tolerable times on a single processor [3, 21-23]. In this research work, the open-source software LIGGGHTS was used to perform DEM simulations. The DEM variant used here is sometimes called a 'soft particle method'. The particles are allowed to overlap, and the extent of overlap is used in conjunction with a contact force law to give instantaneous forces from knowledge of the current positions, orientations, velocities, and spins of the particles [24]. Here, we used the Hertz-Mindlin's contact force law. It states that the repulsive force resulting from a collision is calculated from the amount of normal overlap  $\delta_n$  and tangential overlap  $\delta_t$  (soft-sphere approach) [25]. This granular model uses the following formula for the frictional force between two granular particles when the distance  $r$  between two particles of radii  $R_i$  and  $R_j$  is less than their contact distance  $d = R_i + R_j$ . There is no force between the particles when  $r > d$ :

$$\mathbf{F} = (k_n \delta_n \mathbf{n}_{ij} - \gamma_n \mathbf{v} \mathbf{n}_{ij}) + (k_t \delta_t \mathbf{t}_{ij} - \gamma_t \mathbf{v} \mathbf{t}_{ij}) \quad (1)$$

The first term is the normal force ( $\mathbf{F}_n$ ) between the two particles, and the second term is the tangential force ( $\mathbf{F}_t$ ). The normal force has two terms: a spring force and a damping force. The tangential force also has two terms: a shear force and a damping force. The shear force is a “history” effect that accounts for the tangential displacement (tangential overlap) between the particles for the duration of the time they are in contact.

The quantities in the equation are as follow:

$k_n$ : elastic constant for normal contact;

$\delta \mathbf{n}_{ij}$ :  $d-r$  = normal overlap (overlap distance between two particles);

$\gamma_n$ : viscoelastic damping constant for normal contact;

$\mathbf{v} \mathbf{n}_{ij}$ : normal relative velocity (normal component of the relative velocity of two particles);

$k_t$ : elastic constant for tangential contact;

$\delta \mathbf{t}_{ij}$ : tangential overlap (tangential displacement vector between two spherical particles, which is truncated to satisfy a frictional yield criterion);

$\gamma_t$ : viscoelastic damping constant for tangential contact;

$\mathbf{v} \mathbf{t}_{ij}$ : tangential relative velocity (tangential component of the relative velocity of two particles).

Considering that the shear modulus ( $G$ ) can be calculated from the Young's modulus and Poisson ratio, the Hertz–Mindlin contact model depends on the following material parameters [25]:

Coefficient of restitution,  $e$

Young's modulus,  $Y$

Poisson ratio,  $\nu$

Coefficient of static friction,  $\mu_s$

Coefficient of rolling friction,  $\mu_r$ .

The maximum overlap between particles is determined by the stiffness  $k_n$  of the spring in the normal direction. Typically, average overlaps of 0.1–0.5% are desirable, requiring spring constants of the order of  $10^4$ – $10^6$  N/m in three dimensions. The normal damping coefficient  $\gamma_n$  is chosen to give the required coefficient of restitution  $e$  (defined as the ratio of the post-collisional to the pre-collisional normal component of the relative velocity) [26].

In DEM, particles are traditionally approximated by disks or spheres, in two and three dimensions, respectively. These shapes are preferred due to their computational efficiency. The contact is always on the line joining the center of each particle, and is as simple as comparing the distance between their centers to the sum of their radii [21, 23]. Since in a ball mill the balls are

spherical, DEM can be appropriately used to simulate their movement.

The drawback of DEM is that the time step has to be chosen extremely small because the contact force exhibits a very stiff behavior. Depending on the material properties and the particle size, the time step size can be as low as  $10^{-6}$  s for an accurate simulation [27-29].

## 2.2. SPH method for free surface fluid flow

SPH is a mesh-free or particle-based Lagrangian method for solving systems of partial differential equations. The material is spatially discretized as SPH ‘particles’ using the SPH interpolation process, and the governing partial differential equations are converted to rates of change of state variables stored on the particles. Critically, the solution is solved on these particles, which move with the material flow rather than using any fixed mesh or grid structure. Hence the method is both Lagrangian and mesh-free. Originally developed for astrophysical applications by Gingold and Monaghan [30], it was later extended to solve the Navier–Stokes equations for the flow of incompressible fluids by Monaghan [31]. The method has subsequently been used extensively to predict free surface and industrial fluid flows (see [32-34] for many examples) and for many astrophysical applications (see [32]).

SPH automatically follows complex flows. The Lagrangian nature of SPH means that the numerical diffusion across interfaces (where particles change identity) is absent. This makes the method particularly suited for fluid flows that involve droplet formation, splashing, and complex free surface motion. Although the SPH method is particularly well-suited for high-speed compressible flows, it is able to model a low-speed incompressible flow [35-37].

SPH modelling of free surface fluid flows has been well-established. The basic SPH method has been described in details by Monaghan [38], and its formulation for 3D industrial and geophysical modellings has been given by Cleary et al. [33]. It is a particle-based method for solving the Navier-Stokes equations with complex free surface behaviors in complex moving geometries, and is ideally suited to modelling fluid flow in the tumbling ball mills [12, 39]. The SPH method is based upon the use of local interpolations from the surrounding discrete particles to construct continuous field approximations [12, 39]. This is the basis of the spatial discretization of the governing equations. The interpolated value of a

function A at any position r can be expressed using SPH smoothing as:

$$A(r) = \sum_b m_b \frac{A_b}{\rho_b} W(r - r_b, h) \quad (2)$$

where  $A_b$  is the value of the A function at point b;  $m_b$  and  $\rho_b$  are the mass and density of particle b, and the sum is over all particles b within a radius  $2h$  of r. Here,  $W(r, h)$  is a  $C^2$ -spline-based interpolation or smoothing kernel, which approximates the shape of a Gaussian function but has a compact support with radius  $2h$ .

The gradient of function A is given by differentiating the interpolation Eq. (2) to give:

$$\nabla A(r) = \sum_b m_b \frac{A_b}{\rho_b} \nabla W(r - r_b, h) \quad (3)$$

Using these interpolation formulae and suitable finite difference approximations for second order derivatives, one is able to convert parabolic partial differential equations into ordinary differential equations for the motion of the particles and the rates of change of their properties. The SPH continuity equation, taken from Monaghan (1994), is:

$$\frac{d\rho_a}{dt} = \sum_b m_b (v_a - v_b) \times \nabla W_{ab} \quad (4)$$

where  $\rho_a$  is the density of particle a with velocity  $v_a$ , and  $m_b$  is the mass of particle b. We denote the position vector from particle b to particle a by  $r_{ab} = r_a - r_b$  and let  $W_{ab} = W(r_{ab}, h)$  to be the interpolation kernel with smoothing length  $h$  evaluated for the distance  $|r_{ab}|$ . This form of the continuity equation is Galilean invariant (since the positions and velocities appear only as differences), has good numerical conservation properties, and is not affected by free surfaces or density discontinuities. The use of this form of the continuity equation is very important for predicting free surface flows. The SPH momentum equation becomes [12, 39]:

$$\frac{dv_a}{dt} = g - \sum_b m_b \left[ \left( \frac{P_b}{\rho_b^2} + \frac{P_a}{\rho_a^2} \right) - \frac{\xi}{\rho_a \rho_b} \times \frac{4\mu_a \mu_b}{(\mu_a + \mu_b)} \times \frac{v_{ab} r_{ab}}{r_{ab}^2 + \eta^2} \right] \nabla_a W_{ab} \quad (5)$$

where  $P_a$  and  $\mu_a$  are the pressure and viscosity of particle a and  $v_{ab} = v_a - v_b$ . Here,  $\xi$  is a factor associated with the viscous term,  $\eta$  is a small parameter used to smooth out the singularity at  $r_{ab} = 0$ , and  $g$  is the gravity.

Since the SPH method used here is quasi-compressible, one needs to use an equation of state giving the relationship between particle density and fluid pressure. A suitable one is:

$$P = P_0 \left[ \left( \frac{\rho}{\rho_0} \right)^\gamma - 1 \right] \quad (6)$$

where  $P_0$  is the magnitude of the pressure and  $\rho_0$  is the reference density.  $\gamma = 7$  is suitable for water. This pressure is then used in the SPH momentum equation (Eq. (6)) to give the particle motion. The pressure scale factor  $P_0$  is given by:

$$\frac{\gamma P_0}{\rho_0} = 100V^2 = c_s^2 \quad (7)$$

where  $V$  is the characteristic or maximum fluid velocity. This ensures that the density variation is less than 1% and the flow can be regarded as incompressible.

### 2.3. One-way coupled DEM-SPH model

In general, the softwares that are separately available for both the DEM and SPH methods can be combined and used for coupling if they have the same programming language. In this research work, the open-source software LIGGGHTS (that is a DEM software) and SPHysics (that is a SPH software) were used. LIGGGHTS was used to perform DEM simulations. Also coupling of LIGGGHTS and SPHysics was used to perform combined DEM-SPH simulations.

In this work, a sequential one-way coupling between DEM and SPH was used. This is achieved by averaging the velocity and porosity information from a DEM simulation and using this to characterize the steady state bed as a dynamic porous media, through which the SPH fluid is then able to flow. In this model, particle motion does not affect fluid motion. This approach was chosen since the particulate flow was in the steady state and the balls represented in the DEM were only weakly affected by the slurry motion. Conversely, the slurry motion through the beds is completely dominated by the flow of the balls. This one-way coupling is, therefore, able to capture the dominant interaction between the phases required to predict the slurry behavior. Inclusion of the weaker coupling of the slurry back onto the balls requires a fully coupled DEM-SPH model, and is currently impossible with the existing hardware in this country [38].

The one-way coupling between the DEM and SPH simulations is performed using the following steps:

➤ First, a DEM simulation is run to predict the particle flow and porosity information, which is then spatially averaged onto a Cartesian grid to obtain a volume fraction and velocity distribution that characterizes the coarse particle charge.

➤ Secondly, SPH is used to predict the flow of the fluid and fine slurry component in this charge using a supplied slurry viscosity and a Darcy law porous media drag (Eq. (8)) based on the porosity and velocity distributions from the DEM simulation. The permeability is calculated using the Kozeny-Carman relation (Eq. (9)).

The coupling of the slurry to the porous media is accomplished using a Darcy law drag, which is suitable for modelling porous media. The Darcy drag law is given by:

$$F_{\text{Darcy}} = \varepsilon^2 \mu_a \frac{(V_a - V_{\text{DEM}})}{\rho_a K_{\text{DEM}}} \quad (8)$$

where  $\varepsilon$  is the porosity (void fraction) of the porous media;  $\mu_a$  is the fluid viscosity for SPH fluid particle  $a$ ;  $V_a$  is the velocity of SPH fluid particle  $a$ ;  $V_{\text{DEM}}$  is the DEM solid velocity at that point (interpolated from the grid), and  $\rho_a$  is the fluid density of particle  $a$ .

This force from the Darcy law is added to the standard SPH momentum (Eq. (5)). The SPH method has the advantage that it can easily solve this coupled Navier–Stokes and Darcy law flow problem since its pressure solution is quite robust across the transition from free flowing fluid (where the Navier–Stokes terms dominate) to drag controlled flow in the porous media representing the charge (where the Darcy drag dominates).

The permeability of the porous media at each point of the charge is calculated from the porosity using the Kozeny–Carman equation:

$$K = \frac{\varepsilon^3}{CT(1 - \varepsilon)^2 S^2} \quad (9)$$

where  $K$  is the permeability of the porous media;  $C$  is the shape factor (typically 2–3);  $T$  is the tortuosity of the fluid pathways through the charge, and  $S$  is the ratio of surface area to particle volume (from the DEM particles).

The SPH variables that are solved for are then the:

- pore fluid velocity (or velocity of slurry in the pores of the charge), and
- bulk density of fluid (i.e. the fluid density  $\times$  local porosity).

### 3. Ball mill configuration

In this work, two pilot scale ball mills with no lifter and with eight rectangle lifters were simulated by both DEM and DEM-SPH (Figure 1). These geometries were built from the details estimated from a range of manufacturer website sources and were not intended to correspond to any specific ball mill configuration. This is intended to be a generic ball mill that is suitable for:

- demonstrating the operation of the model in being able to predict slurry and ball flow behavior, and
- to provide general mechanistic information that can enhance broad understanding of effects of lifters on ball shoulder and toe points as well as on creation of cascading and cataracting movements for balls.

The detailed geometrical and operational conditions and material properties for these pilot scale ball mills are listed in Tables 1-3.

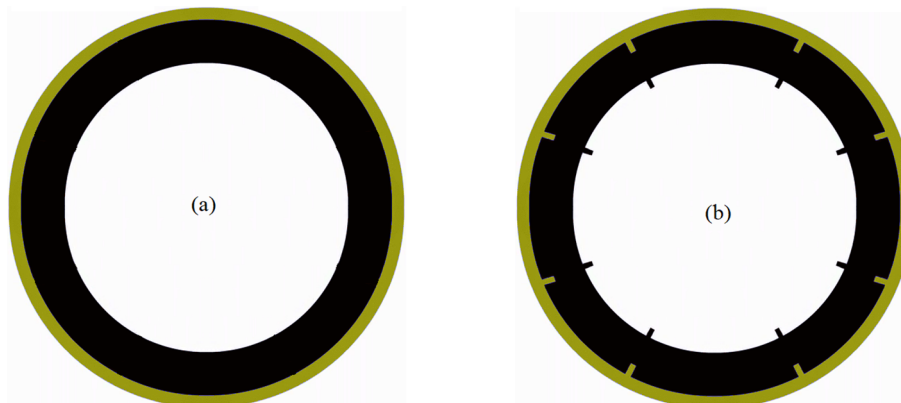


Figure 1. (a) Pilot scale ball mill with no lifter; (b) pilot scale ball mill with eight rectangle lifters.

**Table 1. Ball mill dimensions.**

Pilot scale ball mill	Dimensions
Mill length	5 m
Mill diameter	3 m
Rotation speed	15 rpm
Rotation of mill	Counter-clockwise (as viewed from feed end)
Rectangle lifter length	5 m
Rectangle lifter height	50 mm
Rectangle lifter width	50 mm

**Table 2. DEM ball size distribution.**

Ball size class (mm)	Mass fraction (%)
38 – 40	15
34 – 38	30
30 – 34	30
26 – 30	25

**Table 3. Parameters used for the DEM/SPH simulations of pilot scale ball mills.**

DEM/SPH model details	Value
% Fill of ball charge	35%
# DEM balls in simulation	700,000
Total mass of ball charge	5 tones
DEM spring constant	10 <sup>6</sup> kg/m
Ball density (sg)	7.2
Ball sliding friction coefficient	0.5
Ball rolling friction coefficient	0.01
Poisons ratio	0.45
Young's modulus (N/m <sup>2</sup> )	5×10 <sup>5</sup>
Ball restitution coefficient	0.6
#SPH fluid particles	875,000
Initial fluid volume in mill	4,200 L
SPH particle separation	8 mm
SPH sound speed	4 m/s
Fluid density (sg)	1.8
Fluid viscosity	300 cP

**4. Results and discussion**

Figure 2 demonstrates snapshots of the simulations of the pilot scale ball mill with no lifter using DEM and DEM-SPH, respectively. Also Figure 3 demonstrates snapshots of the simulations of the pilot scale ball mill with eight lifters using the DEM and DEM-SPH coupling methods, respectively. As already mentioned, in DEM, only the solid phase (balls) is simulated but in the DEM-SPH method, both the solid phase and fluid phase (balls/slurry) are simulated, that is, the effect of the fluid phase on the movement of the balls is also simulated. Figure 4 demonstrates the height (m) and angle (degree) of the shoulder and toe points in the pilot scale ball mill with no lifter. It also shows that there is only cascading movements, and shows that in dry

condition (DEM), the shoulder point is higher than that in the couple condition (DEM-SPH); however, the toe point in a dry condition is lower than that in the wet condition. It can be concluded that the fluid phase causes the balls to rise to a lower height, and as a result, the grinding will not be done properly. Therefore, it is necessary that the speed of the mill in the wet state is slightly increased. Also Figure 5 demonstrates the height and angle of the shoulder and toe points in the pilot scale ball mill with eight lifters. It shows that there are both cascading and cataracting movements, and therefore, grinding in this case will be better than in Figure 4, i.e. the no-lifter mode. The same as Figure 4, it also demonstrates that in dry condition (DEM), the shoulder point is higher than that in the couple condition (DEM-SPH); however, the toe point in a dry condition is lower than that in the wet condition. It can be concluded that in this case, also the fluid phase causes the balls to rise to a lower height, and as a result, the grinding will not be done properly. Therefore, it is necessary that the speed of the mill in the wet state is slightly increased. In general, it can be said that in order to eliminate the adverse effect of the fluid phase on grinding, the mill speed should be slightly increased relative to the dry state. The exact values for the height and angle of the shoulder and toe points of the balls are visible in both dry and wet conditions for no-lifter and eight-lifter mills in Table 4. In the first glance, the results shown in Figures 3-5 and Table 4 may seem simple software outputs from DEM and SPH. However, after simulations, all the required information is available on the motion of particles and fluid properties so that the researcher (computer user) can examine the position of each individual particle and the effect of the fluid phase on its movement, which leads to the identification of charge shoulder and toe points, which was the main purpose of this work.

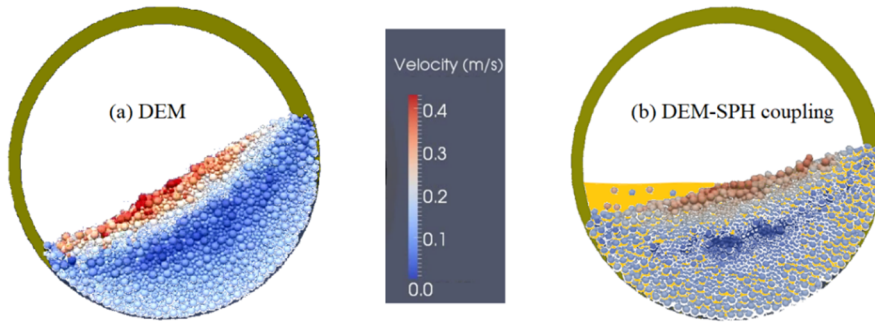


Figure 2. Snapshots showing the motion of particles on the pilot scale ball mill with no lifter (a) using DEM simulation method (single solid phase); (b) using DEM-SPH coupling method (two phase). The fluid is transparent and orange, while the particles are colored by their speed.

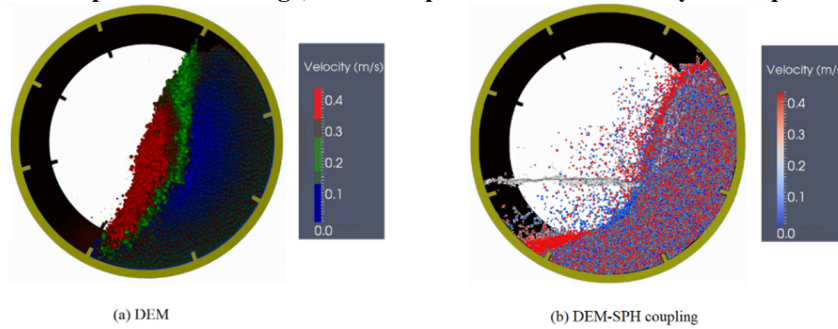


Figure 3. Snapshots showing the motion of particles on the pilot scale ball mill with eight lifters (a) using DEM simulation method (single solid phase); (b) using DEM-SPH coupling method (two phase). The fluid is transparent and pale gray, while the particles are colored by their speed.

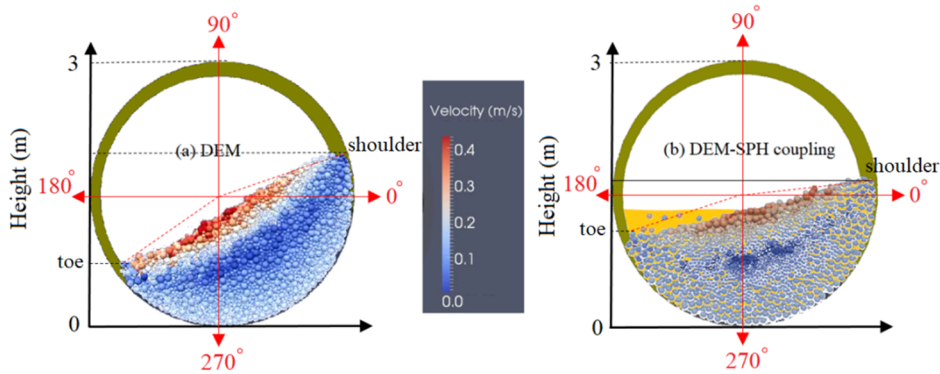


Figure 4. Determining the height (m) and angle (degree) of the shoulder and toe points in the pilot scale ball mill with no lifter (a) using DEM simulation method (single solid phase); (b) using DEM-SPH coupling method (two phase). The fluid is transparent and orange, while the particles are colored by their speed.

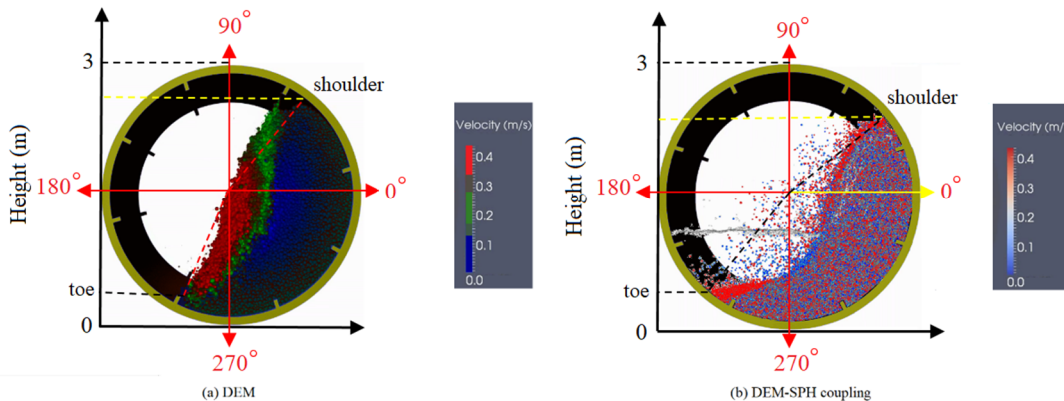


Figure 5. Determining the height (m) and angle (degree) of the shoulder and toe points in the pilot scale ball mill with eight lifters (a) using DEM simulation method (single solid phase); (b) using DEM-SPH coupling method (two phase). The fluid is transparent and pale gray, while the particles are colored by their speed.

**Table 4. Values for the height and angle of the shoulder and toe points of the balls in both dry and wet conditions for no-lifter and eight-lifter ball mills.**

Mill Type	Cascade movement	Cataract movement	Shoulder height (m)	Toe height (m)	Shoulder angle (degree)	Toe angle (degree)
No-lifter dry	yes	no	2.00	0.72	19.36	214.16
No-lifter wet	yes	no	1.72	1.08	6.17	197.35
8-lifter dry	yes	yes	2.62	0.38	51.84	244.18
8-lifter wet	yes	yes	2.37	0.44	39.40	230.19

**4.1. Need for validation**

The aim of this paper was to propose and demonstrate a numerical scheme based on one-way coupling of the DEM and SPH methods for modelling dense slurries interacting with coarse particulates (here, balls) for complex industrial process applications. At the present time, there is little in the way of measured data for such flows available in the public domain that can be used to adequately validate these types of predictions. This means that the results presented here are necessarily somewhat speculative [40]. To use these methods with confidence for process design and optimization requires a detailed comparison with experiment. Small-scale laboratory experiments can be selectively measured using PEPT, and are expected to be one source of such validation. However, experimental visualizations for flow within the grinding chamber and discharge from ball mills with diameters around 1 m are also highly desirable. Such measurements are very difficult and expensive, and so are expected to limit the rate at which these coupled models can be sufficiently validated [40].

The key issues that would be illuminated by comparisons of these simulation predictions with a good experiment include:

1. Determining the functional nature and the scaling of the coupling forces between phases.
2. Impact of the averaging of data to produce the solid and fluid fractions and the phase velocities that are the inputs to the coupling force calculations.
3. Impact of the interstitial fluid on the contact mechanics and the consequent changes in the effective contact mechanical properties [40].

**5. Conclusions**

In this research work, an open-source software LIGGGHTS (which is a DEM software) and SPHysics (which is a SPH software) were used. LIGGGHTS was used to perform the DEM simulations. Also coupling of LIGGGHTS and SPHysics was used to perform the combined DEM-SPH simulations. The following results were obtained:

- In the pilot scale, ball mill with no lifter, there is only cascading movements as well as in dry condition (DEM) the shoulder point is higher than that in the couple condition (DEM-SPH); however, the toe point in a dry condition is lower than that in the wet condition.

- In the pilot scale ball mill with no lifter, the fluid phase causes the balls to rise to a lower height, and as a result, it can affect the grinding process. Therefore, in order to compute ball mill power draw, DEM alone is not enough and DEM-SPH coupling should be used.

- In the pilot scale ball mill with eight lifters, there are both cascading and cataracting movements, and therefore, grinding in this case will be better than the no-lifter mode.

- The same as the no-lifter mode, in dry condition (DEM), the shoulder point is higher than that in the wet condition (DEM-SPH); however, the toe point in a dry condition is lower than that in the wet condition.

- Also in the 8-lifter case, the fluid phase causes the balls to rise to a lower height, and as a result, it can affect the grinding process. Therefore, in order to compute ball mill power draw, DEM alone is not enough and DEM-SPH coupling should be used.

- In general, it can be said that in order to more exactly compute the ball mill power draw, DEM alone is not enough and DEM-SPH coupling should be used. In other words, the DEM-SPH coupling results are more reliable.

- Finally, the results obtained indicated that fluid slurry in the mill lowered the charge shoulder by about 28 cm and 25 cm in the no-lifter and eight-lifter cases, respectively. However, it raised the charge toe by about 36 cm and 6 cm in the no-lifter and eight-lifter cases, respectively.

**References**

[1]. Pedrayes, F., Normiella, J.G., Melero, M.G., Menéndez-Aguado, J.M., Juan, J.J. and del Coz-Díaz, J. (2018). Frequency domain characterization of torque in tumbling ball mills using DEM modelling: Application to filling level monitoring. Powder Technology. 323: 433-444.

- [2]. Wills, B.A. and Napier-Munn, T.J. (2016). Wills' Mineral Processing Technology. 8<sup>th</sup> edition. Elsevier. pp. 147-180.
- [3]. Cleary, P.W. (2004). Large scale industrial DEM modeling. *Eng. Comput.* 21: 169-204.
- [4]. Cleary, P.W., Sinnott, M.D. and Morrison, R.D. (2008). DEM prediction of particle flows in grinding processes. *Int. J. Numer. Methods Fluids.* 58: 319-353.
- [5]. Cleary, P.W. (2009). Ball motion, axial segregation and power consumption in a full scale two chamber cement mill. *Miner. Eng.* 22: 809-820.
- [6]. Kozicki, J. and Donzé, F.V. (2009). YADE-OPEN DEM: an open-source software using a discrete element method to simulate granular material. *Eng. Comput.* 26: 786-805.
- [7]. Chen, J., Huang, B., Chen, F. and Shu, X. (2012). Application of discrete element method to Superpave gyratory compaction. *Road materials and pavement design.* 13: 480-500.
- [8]. Zhang, L., Quigley, S.F. and Chan, A.H.C. (2013). A fast scalable implementation of the two-dimensional triangular Discrete Element Method on a GPU platform. *Adv. Eng. Softw.* 60-61: 70-80.
- [9]. Kruggel-Emden, H., Sturm, M., Wirtz, S. and Scherer, V. (2008). Selection of an appropriate time integration scheme for the discrete element method (DEM). *Comput. Chem. Eng.* 32: 2263-2279.
- [10]. Cleary, P.W. and Morrison, R.D. (2012). Prediction of 3D slurry flow within the grinding chamber and discharge from a pilot scale SAG mill. *Minerals Engineering.* 39: 184-195.
- [11]. Cleary, P.W., Sinnott, M. and Morrison, R. (2006). Prediction of slurry transport in SAG mills using SPH fluid flow in a dynamic DEM based porous media. *Minerals Engineering.* 19: 1517-1527.
- [12]. Sinnott, M.D., Cleary, P.W. and Morrison, R.D. (2017). Combined DEM and SPH simulation of overflow ball mill discharge and trommel flow. *Minerals Engineering.* 108: 93-108.
- [13]. Nassauer, B., Liedke, T. and Kuna, M. (2013). Polyhedral particles for the discrete element method. *Granular Matter.* 15 (1): 85-93.
- [14]. Raji, A.O. and Favier, J.F. (2004). Model for the deformation in agricultural and food particulate materials under bulk compressive loading using discrete element method. I: theory, model development and validation. *J. Food Eng.* 64: 359-371.
- [15]. Nassauer, B. and Kuna, M. (2013). Contact forces of polyhedral particles in discrete element method. *Granul. Matter.* 15: 349-355.
- [16]. Balevičius, R., Džiugys, A., Kačianauskas, R., Maknickas, A. and Vislavičius, K. (2006). Investigation of performance of programming approaches and languages used for numerical simulation of granular material by the discrete element method. *Comput. Phys. Commun.* 175: 404-415.
- [17]. Delaney, G.W., Cleary, P.W., Morrison, R.D., Cummins, S. and Loveday B. (2013). Predicting breakage and the evolution of rock size and shape distributions in Ag and SAG mills using DEM. *Miner. Eng.* 50-51: 132-139.
- [18]. Ting, J.M., Khwaja, M., Meachum, L.R. and Rowell, J.D. (1993). An ellipse-based discrete element model for granular materials. *Int. J. Numer. Anal. Methods Geomech.* 17: 603-623.
- [19]. Shmulevich, I. (2010). State of the art modeling of soil-tillage interaction using discrete element method. *Soil Tillage Res.* 111: 41-53.
- [20]. Cleary, P.W. and Sawley, M.L. (2002). DEM modelling of industrial granular flows: 3D case studies and the effect of particle shape on hopper discharge. *Appl. Math. Model.* 26: 89-111.
- [21]. Cleary, P.W. (2009). Industrial particle flow modelling using discrete element method. *Eng. Comput.* 26: 698-743.
- [22]. Cleary, P.W. and Sinnott, M.D. (2008). Assessing mixing characteristics of particle-mixing and granulation devices. *Particuology.* 6: 419-444.
- [23]. Cleary, P.W. (2010). DEM prediction of industrial and geophysical particle flows. *Particuology.* 8: 106-118.
- [24]. Cleary, P.W. and Morrison, R.D. (2009). Particle methods for modelling in mineral processing. *Int. J. Comput. Fluid Dyn.* 23: 137-146.
- [25]. Just, S., Toschkoff, G., Funke, A., Djuric, D., Scharrer, G., Khinast, J., Knop, K. and Kleinebudde, P. (2013). Experimental analysis of tablet properties for discrete element modeling of an active coating process. *AAPS PharmSciTech.* 14: 402-411.
- [26]. McBride, W. and Cleary, P.W. (2009). An investigation and optimization of the 'OLDS' elevator using Discrete Element Modeling. *Powder Technol.* 193: 216-234.
- [27]. Goniva, C., Kloss, C., Deen, N.G., Kuipers, J.A.M. and Pirker, S. (2012). Influence of rolling friction on single spout fluidized bed simulation. *Particuology.* 10: 582-591.
- [28]. Goniva, C., Kloss, C., Hager, A. and Pirker, S. (2010). An open source CFD-DEM perspective, *Proceedings of OpenFOAM Workshop Gothenburg, Sweden.*
- [29]. Kloss, C., Goniva, C., Aichinger, G. and Pirker, S. (2009). Comprehensive DEM-DPM-CFD simulations-model synthesis, experimental validation and scalability, *Seventh International Conference on CFD in the Minerals and Process Industries CSIRO, Melbourne, Australia.*

- [30]. Gingold, R.A. and Monaghan, J.J. (1977). Smoothed particle hydrodynamics, theory and application to non-spherical stars. *Monthly notices of the royal astronomical society*. 181 (3): 375-389.
- [31]. Monaghan, J.J. (1992). Smoothed particle hydrodynamic. *Annu. Rev. Astron. Astrophys.* 30: 543-574.
- [32]. Monaghan, J.J. (2005). Smoothed particle hydrodynamics. *Rep. Prog. Phys.* 68: 1703-1759.
- [33]. Cleary, P.W., Prakash, M., Ha, J., Stokes, A.N. and Scott, C. (2007). Smoothed particle hydrodynamics: status and future potential. *Prog. Comput. Fluid Dyn.* 7: 70-90.
- [34]. Cleary, P.W. (2010). Elastoplastic deformation during projectile-wall collision. *Applied Mathematical Modelling*. 34: 266-283.
- [35]. Cummins, S.J. and Rudman, M. (1999). An SPH projection method. *J. Comp. Phys.* 152: 584-607.
- [36]. Morris, J.P., Fox, P.J. and Zhu, Y. (1997). Modeling low Reynolds number incompressible flows using SPH. *J. Comput. Phys.* 136: 214-226.
- [37]. Cleary, P., Ha, J., Alguine, V. and Nguyen, T. (2002). Flow modelling in casting processes. *Applied Mathematical Modelling*. 26: 171-190.
- [38]. Monaghan, J.J. (1994). Simulating free surface flows with SPH. *Journal of Computational Physics*. 110: 399-406.
- [39]. Fernandez, J.W., Cleary, P.W., Sinnott, M.D. and Morrison, R.D. (2011). Using SPH one-way coupled to DEM to model wet industrial banana screens. *Minerals Engineering*. 24: 741-753.
- [40]. Cleary, P.W. (2015). Prediction of coupled particle and fluid flows using DEM and SPH. *Minerals Engineering*. 73: 85-99.

## شبیه‌سازی تلفیقی DEM و SPH آسیاکنی گلوله‌ای

محمد جهانی چگنی

دانشکده مهندسی معدن، نفت و ژئوفیزیک، دانشگاه صنعتی شاهرود، ایران

ارسال ۲۰۱۸/۸/۱۳، پذیرش ۲۰۱۸/۱۱/۱۳

نویسنده مسئول مکاتبات: m.jahani1983@gmail.com

### چکیده:

درک عمیق‌تر عملیات آسیاکنی آسیاهای گلوله‌ای به مهندسان فرآوری مواد معدنی کمک می‌کند تا آن‌ها را کنترل و بهینه‌سازی کنند و در نتیجه، توان مصرفی آن‌ها را کاهش دهند. در این پژوهش، عملیات آسیاکنی آسیاهای گلوله‌ای با استفاده از دو روش یعنی DEM و DEM-SPH تلفیقی مورد بررسی قرار گرفته است. ابتدا، یک آسیای گلوله‌ای مقیاس پایلوت بدون هیچ لیفتری به وسیله هر دو روش شبیه‌سازی شده است. سپس، یک آسیای گلوله‌ای مقیاس پایلوت دیگر با هشت لیفتر مستطیل شکل دوباره به وسیله هر دو روش شبیه‌سازی شده است. اثرات لیفترها بر نقاط شانه و پاشنه بار و نیز ایجاد حرکات آبشاری کوچک و بزرگ برای گلوله‌ها به وسیله هر دو روش مورد بررسی قرار گرفته‌اند. در حال حاضر، داده‌های اندازه‌گیری شده کافی موجود برای دوغاب‌های چگالی که با ذرات دانه‌ای درشت موجود در حوزه عمومی اندرکنش می‌کنند، وجود ندارند تا بتوانند به طور مناسب برای اعتبار بخشیدن به این نوع از پیش‌بینی‌ها مورد استفاده قرار گیرند. نتایج به دست آمده نشان دادند که دوغاب سیال در آسیا شانه بار را به ترتیب تا حدود ۲۸ سانتی‌متر و ۲۵ سانتی‌متر در حالت‌های بدون لیفتر و هشت لیفتری پایین برده است. با وجود این، دوغاب سیال پاشنه بار را به ترتیب تا حدود ۳۶ سانتی‌متر و ۶ سانتی‌متر در حالت‌های بدون لیفتر و هشت لیفتری بالا برده است.

**کلمات کلیدی:** شبیه‌سازی، آسیای گلوله‌ای، روش اجزای گسسته، هیدرودینامیک ذرات هموار، کوپل DEM-SPH.